Comparison of SVM kernels in brain tumor image classification using GLCM feature extraction

Kraugusteeliana Kraugusteeliana [a,1], I Gede Susrama Mas Diyasa [b,2,*], Hanif Nur Fadlilah [b,3], Yisti Vita Via [b,4], Anita Muliawati [a,5], Allan Ruhui Fatmah Sari [b,6], Erna Harfiani [c,7], Ni Made Ika Marini Mandenni [d,8], Deshinta Arrova Dewi [e,9]

[a] Department of Information Systems, Faculty of Computer Science, University of Pembangunan Nasional "Veteran" Jakarta, Jakarta, Indonesia
[b] Department of Informatics, Faculty of Computer Science, University of Pembangunan Nasional "Veteran" Jawa Timur, Surabaya, Indonesia
[c] Department of Medicine, Faculty of Medicine, University of Pembangunan Nasional "Veteran" Jakarta, Jakarta, Indonesia
[d] Department of Information Technology, Udayana University, Denpasar, Bali, Indonesia
[e] Center for Data Science and Sustainable Technologies, INTI International University, Malaysia
[1] kraugusteeliana@upnvj.ac.id; [2] igsusrama.if@upnjatim.ac.id; [3] 20081010231@student.upnjatim.ac.id; [4] yistivia.if@upnjatim.ac.id; [5] anitamuliawati@upnvj.ac.id; [6] allanruhui@gmail.com; [7] ernaharfiani@upnvj.ac.id; [8] made_ikamarini@unud.ac.id; [9] deshinta.ad@newinti.edu.my
* corresponding author

ARTICLE INFO

Article history
Received June 13, 2025
Revised February 12, 2026
Accepted March 1, 2026
Available Online May 31, 2026

Keywords
Brain Tumor
GLCM-SVM
Classification
Cancer
Public Health

ABSTRACT

The human brain plays a vital role in regulating bodily functions, and abnormal cell growth may lead to life-threatening brain tumors. Automated computer-aided diagnosis systems are therefore essential to support early detection from MRI images. This study investigates brain tumor classification using Gray Level Co-occurrence Matrix (GLCM) feature extraction combined with Support Vector Machine (SVM) classification. Unlike prior works that typically employ a single kernel configuration, this study conducts a systematic comparison of four SVM kernels: linear, polynomial, radial basis function (RBF), and sigmoid under a consistent preprocessing pipeline and structured hyperparameter tuning framework. GLCM features, including energy, contrast, correlation, and homogeneity, were extracted at multiple distances and angles. Kernel performance was evaluated using controlled hyperparameter search procedures to ensure fair comparison across models. Experimental results on a binary MRI dataset consisting of 2,800 images demonstrate that the RBF kernel achieved the highest accuracy of 96% with C = 100 and gamma = 10, outperforming polynomial (74%), linear (72%), and sigmoid (71%) kernels. The findings highlight the importance of systematic kernel evaluation and parameter sensitivity analysis in texture-based medical image classification. The proposed GLCM–SVM framework provides a computationally efficient and interpretable approach that may support preliminary decision-aid systems for brain tumor screening.

1. Introduction

As the central organ of the nervous system, the brain regulates all bodily functions [1], [2] This incredibly complex organ, composed of over 100 billion cells, can develop abnormal growths known as brain tumors [3], [4], [5], [6] These tumors originate from the unregulated growth of cells in or around the brain. Brain tumors occur when brain cells grow abnormally within the brain. Brain tumor patients experience a variety of focal and general symptoms. Brain tumors are the tenth leading cause of mortality for both males and females [7]. The annual mortality rate from brain tumors is 4.25 per 100,000 individuals, and the global incidence of brain tumors continues to rise each year [7].

Various computer vision technologies, including face recognition and tumor detection, have been widely developed in recent years to automate object identification in digital images. One of the most impactful applications is in the field of medical image analysis, which supports early disease diagnosis such as brain tumor detection [8]. Medical image analysis is one of many methods employed for early detection [9], [10]. While X-rays and CT scans provide limited information, MRI scans offer high-quality images that can clearly distinguish between soft and hard tissues in the brain, making them highly sensitive for detecting brain tumors [11], [12], [13], [14]. While manual diagnosis relies on biopsy and direct observation of brain tumors, these methods are time-consuming due to laboratory processing and prone to human error [15]. Consequently, automated computer-aided diagnosis offers a more efficient solution for clinicians.

In previous works, AI has also been used to model nonlinear systems and classify emotional patterns from text, showing the flexibility of machine learning methods in various domains [16]. Previous research by Ghazvini et al. [17] discussed the classification of brain tumor types based on glioma images using the Support Vector Machine method. This study employed the SVM algorithm to categorize glioma and meningioma images. The methodology involved data collection from the Kaggle benchmark, preprocessing (scaling and grayscale conversion), segmentation using binary thresholding, feature extraction using the GLCM, and a classifier using SVM with a linear kernel. The model was evaluated on a dataset of 100 images (50 for each class), with 24 images used for testing. The results demonstrated a promising accuracy of 91% in classifying brain tumor types.

Another study by Farghaly and Deshpande (2024) focused on classifying COVID-19 cases using texture-based features, including Gray Level Co-occurrence Matrix (GLCM), combined with conventional machine learning classifiers such as Support Vector Machine (SVM), applied to chest X-ray images [18]. The dataset was collected from publicly available sources and consisted of COVID-19, viral pneumonia, and normal chest X-ray images. The research process involved image acquisition, preprocessing, texture feature extraction using GLCM, classification using SVM, and performance evaluation. The results demonstrated that the SVM-based approach achieved high classification accuracy in distinguishing COVID-19 from other respiratory conditions, highlighting the effectiveness of texture-based machine learning methods in medical image analysis.

Research conducted by Li et al. [19], discussed facial expression recognition using machine learning approaches, including texture-based feature extraction methods such as Gray Level Co-occurrence Matrix (GLCM). In this study, facial images were processed to extract texture features that represent variations in facial patterns associated with different expressions. These features were then classified using machine learning algorithms to identify basic facial expressions. The findings indicated that texture-based methods can effectively capture facial expression characteristics, although the recognition accuracy varied across different expression categories.

The application of AI in healthcare parallels its expanding use in human resource and organizational performance domains [20]. Based on previous studies, this research employs a three-step process for brain tumor classification. The process begins with preprocessing and feature extraction using the Gray Level Co-occurrence Matrix (GLCM) to extract information from each MRI image. The extracted GLCM features include energy, contrast, homogeneity, and correlation. The final step is classification using Support Vector Machine (SVM). SVM is selected due to its superior ability to handle classification problems by finding the optimal hyperplane between classes and controlling decisions based on the chosen kernel [21]. In this study, linear, RBF, polynomial, and sigmoid kernels are utilized. The combination of these methods is expected to yield more accurate classification results.

Previous studies applying GLCM–SVM for medical image classification often vary considerably in terms of dataset size, number of MRI samples, preprocessing techniques, and selected GLCM parameter configurations such as angle and distance. Some works evaluate a single kernel without systematic comparison, while others apply different experimental splits or limited hyperparameter exploration. These methodological differences make it difficult to directly compare reported accuracy values across studies and reduce the clarity of kernel-specific performance behavior [22], [23].

Despite numerous studies applying GLCM and SVM for brain tumor image classification, many of them differ in preprocessing strategies, hyperparameter search spaces, and evaluation protocols, making direct comparison difficult. The primary contribution of this study is not merely identifying the best-performing kernel, but establishing a structured and controlled comparison framework to systematically evaluate SVM kernel behavior under identical preprocessing, feature extraction, and hyperparameter tuning conditions for brain tumor MRI classification. All kernels are evaluated using the same preprocessing pipeline, GLCM feature configuration, and hyperparameter search framework to ensure methodological fairness. Furthermore, this research investigates the impact of GLCM distance and angle configurations on classification performance while implementing reproducible hyperparameter optimization using GridSearchCV with a fixed train–test split. By emphasizing experimental consistency, transparency, and robustness, this work positions itself as a methodological benchmark rather than simply reporting the highest accuracy.

To the best of our knowledge, limited studies have explicitly combined structured GridSearch-based hyperparameter optimization with systematic SVM kernel comparison under identical GLCM preprocessing conditions for brain tumor MRI classification. While prior works have employed GLCM features and SVM classifiers, many focus primarily on reporting accuracy outcomes without detailing controlled cross-kernel evaluation or reproducible hyperparameter search strategies. The present study contributes by integrating these components within a unified and transparent experimental framework.

2. Method

This study employs a structured experimental framework to evaluate the performance of Support Vector Machine (SVM) kernels for brain tumor MRI classification using texture-based feature extraction. The overall workflow of the proposed approach is illustrated in Fig. 1. The framework consists of five main stages: dataset preparation, preprocessing, feature extraction using Gray Level Co-occurrence Matrix (GLCM), kernel-based SVM classification with hyperparameter tuning, and performance evaluation.

The research begins with the acquisition of a 2,800-image MRI dataset categorized into tumor and non-tumor classes. A preprocessing stage is subsequently applied to standardize image inputs and enhance feature consistency. Texture features are then extracted using GLCM, focusing on four statistical descriptors: energy, contrast, correlation, and homogeneity. These features are used as input to SVM classifiers with four different kernel functions: linear, polynomial, radial basis function (RBF), and sigmoid, under controlled hyperparameter search procedures. Finally, model performance is evaluated using confusion matrix-based metrics to ensure consistent and fair comparison across kernels.

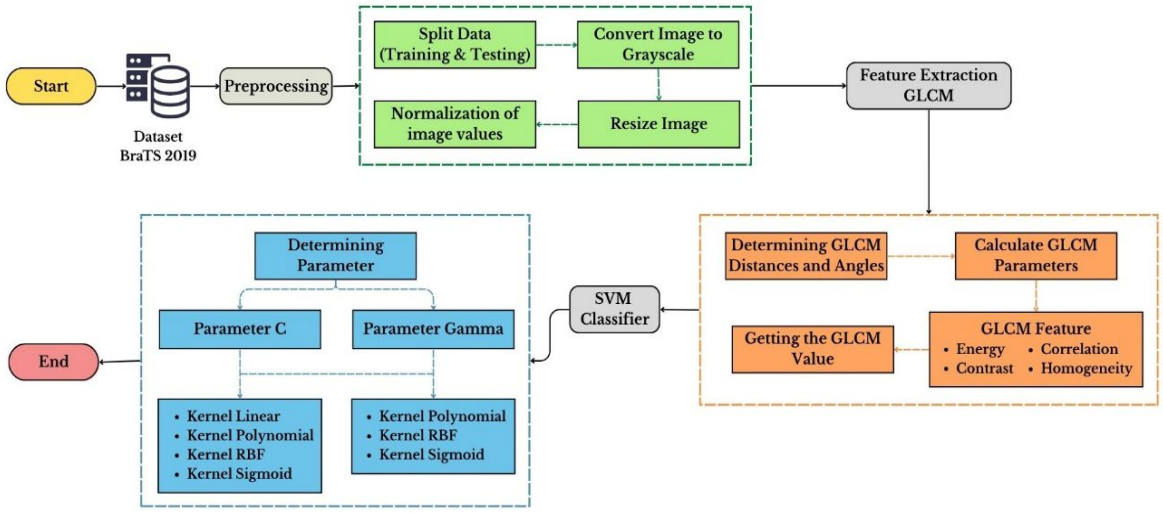

Fig. 1. Overview of the proposed research workflow for GLCM-based feature extraction and SVM kernel comparison in brain tumor MRI classification.

2.1. Dataset Collection

The dataset used in this study was obtained from the Kaggle repository titled *"BraTS 2019 (Train/Test/Valid)"* uploaded by Aryan Felix. This dataset represents a reorganized version of MRI slices derived from the BraTS 2019 collection and has been structured for binary classification purposes, where images are categorized into two folders: "yes" (tumor) and "no" (non-tumor), as seen in Fig. 1. It is important to emphasize that this study does not directly use the original BraTS 2019 segmentation challenge dataset. Instead, it utilizes the binary-class version provided on Kaggle. The dataset consists of 2,800 MRI images, comprising 1,400 tumor and 1,400 non-tumor images. The labels provided in the Kaggle repository were adopted as-is without additional modification, and no segmentation masks were used in this study.

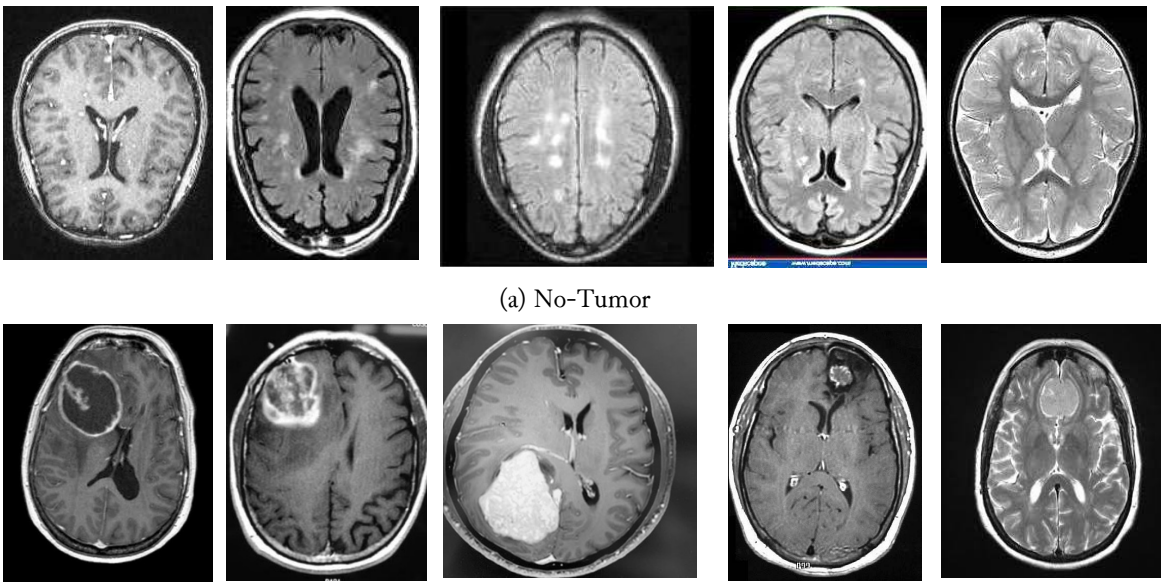

(a) No-Tumor

(b) Tumor

Fig. 2. Representative MRI slices from the Kaggle "BraTS 2019 (Train/Test/Valid)" dataset structured for binary classification: (a) Non-tumor images and (b) Tumor images.

Fig. 2 illustrates representative examples from both classes. The non-tumor images show normal anatomical brain structures without abnormal mass formations, whereas the tumor images exhibit visible irregular tissue regions and abnormal intensity patterns characteristic of tumor presence. These variations in texture and intensity distribution motivate the use of texture-based feature extraction methods such as GLCM for distinguishing between the two classes.

2.2. Preprocessing

Prior to image classification, all images undergo a preprocessing stage. Preprocessing is the initial step taken to improve image quality and facilitate subsequent analysis or information extraction. The main objectives of preprocessing include noise reduction, image enhancement, object segmentation, and simplification of subsequent processes [24]. By simplifying the image data, the preprocessing stage contributes to improved accuracy and efficiency in classification tasks.

The preprocessing stage begins with data partitioning, where 20% of the dataset is allocated for testing and 80% for training. The dataset was partitioned using a fixed random_state parameter to ensure reproducibility and consistency of the train–test split across experimental runs. Next, color space conversion is performed to convert the images from RGB color space to grayscale representation, thereby reducing the dimensions and computational complexity. To cope with variations in image size, all images were resized to the standard dimension of 192x192 pixels. This dimension was chosen because it is considered to be a good match between computational efficiency and preserving image details. Finally,

Min-Max normalization was applied to rescale pixel intensities from the original range of 0-255 to 0-1, facilitating a more uniform distribution of values.

2.3. Feature Extraction

This research study the Gray Level Co-occurrence Matrix (GLCM) technique for the extraction of image texture features [22], [25]. It is a mathematical model that defines the spatial relationship between pixel pairs with specific intensities in an image. The GLCM is a 2D matrix that counts the frequency of pixel pairs with specific intensities at a given distance and angle. GLCM provides information about the interaction between pixel intensities in an image, enabling more detailed texture analysis. Precise tracking and extraction of spatial features are critical to ensure discriminative texture representation, a concept also supported by findings in motion analysis using hybrid approaches such as Kalman filters [26].

In this study, the feature extraction process using GLCM starts with another image preprocessing step to improve the accuracy of the data. The integration of interactive visual representations has shown to enhance pattern recognition in digital systems [27]. Next, GLCM parameters such as distance and angle are determined. Calculations are performed for each parameter combination. This research uses GLCM matrix parameters with angles of 0°, 45°, 90°, and 135°, and distances of 1, 2, and 3 pixels [25], [28]. The purpose of using various distances and angles is to identify the optimal combination that will improve classification accuracy. For each pixel, the frequency of occurrence of pairs of pixels with corresponding intensities was calculated and entered into the GLCM matrix. Next, various GLCM features are extracted. In this study, four features are used: energy, contrast, correlation, and homogeneity [29].

- Energy

  Energy (E) is a feature that reflects the intensity level of pixels in an image, with higher energy values signifying greater similarity between the pixels [30]. Energy can be calculated using Equation 1:

$$E = \sum_x \sum_y P\,(x,y)^2 \tag{1}$$

- Contrast

  Contrast (I) is a feature that measures the difference between two or more images, whether the difference is caused by brightness or color variations in each image [30]. Contrast can be calculated using Equation 2:

$$I = \sum_x \sum_y (x,y)^2\, P(x,y) \tag{2}$$

- Correlation

  Correlation (C) is a feature that evaluates the relationship between gray levels of pixel pairs in an image, reflecting the correlation between the linear grayscale and the level of similarity [30]. Correlation can be calculated using Equation 3:

$$C = \frac{\sum_x \sum_y (x-\mu_s)(y-\mu_v) * P(x,y)}{\sigma_s \sigma_v} \tag{3}$$

- Homogeneity

  Homogeneity (H) is a feature that describes the degree of similarity between gray levels in an image. The more similar the pixels in an image, the higher the homogeneity value [30]. Homogeneity can be calculated using Equation 4:

$$H = \sum_x \sum_y \frac{1}{1+|x-y|^2} P(x,y) \tag{4}$$

After the process is complete, the GLCM values or patterns and angular distance combinations obtained from each image will be transformed. Each image that has a new pattern will have a different

GLCM value. Each of these features provides specific information about the texture pattern of the image that can be used in the classification process.

2.4. Classification

SVM (Support Vector Machine) is a widely used machine learning algorithm for image processing tasks, including classification and regression [31]. The algorithm works by finding the best decision boundary or hyperplane that can divide the n-dimensional space into classes, thus enabling rapid classification of new data. The hyperplane itself is a function that acts as a separator between classes. It is obtained from finding the support vector or the outermost data point of a class. The outermost data type is used as a reference to create a dividing line, called a hyperplane, so as to separate different classes. In image processing, SVMs are used to classify images based on features extracted from the image. SVMs can be categorized into two types: Linear SVMs and non-linear SVMs [31]. Linear SVMs are employed for data that can be divided into two classes using a straight line, and these are referred to as linear SVM classifiers. On the other hand, a non-linear SVM is used for data that cannot be separated by a straight line or datasets that cannot be classified linearly [32]. For the data in this study, a non-linear SVM classifier is used.

The SVM classification process begins by inputting training data to train the classification model. Training is conducted by experimenting with various kernels and SVM parameters to determine the optimal combination for the given dataset. The kernels used are: sigmoid, linear, polynomial, and RBF (Radial Basis Function), each with different mathematical properties that influence the decision boundary [32], [33], [34]. The parameters used include: C, which manages the balance between maximizing the margin and minimizing training errors; gamma, which defines the impact of a single training example; and degree, which specifies the polynomial order of the polynomial kernel [30]. By tuning these parameters, the model's performance can be optimized for the specific classification task. This process is similar to quality assurance efforts in software development, where parameter tuning ensures optimal system performance [35].

- Linear Kernel

  The linear kernel is used to analyze linearly separable data and has many features for various types of data [30]. The linear kernel can be calculated using Equation 5.

$$K(x, x^2) = x^T x^i \tag{5}$$

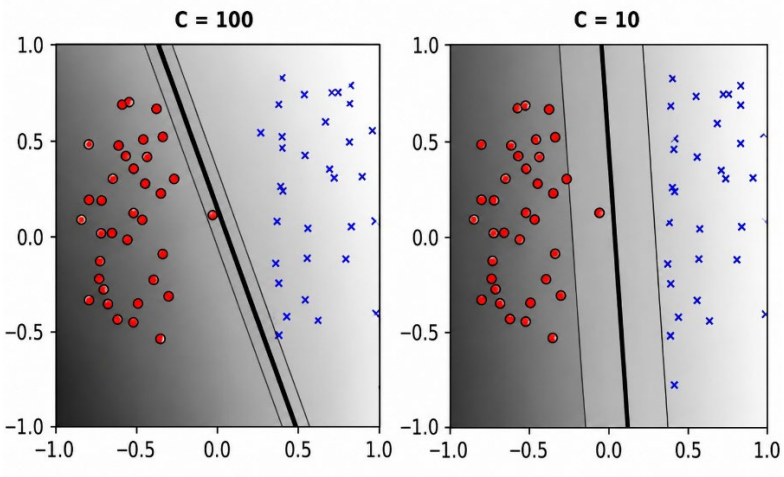

Fig. 3. Linear Kernel [26].

Fig. 3 shows that a low value of C(10) results in wide margins with small error margins, and tends to ignore points near the decision boundary. In contrast, a high value of C(100) narrows the margin and results in a larger margin of error [36], [37], [38].

- Polynomial Kernel

  The polynomial kernel is applied to non-linear data to address problems once all the training data has been normalized. The polynomial kernel is calculated using Equation 6.

$$K(x, x^{\mathrm{i}}) = (\mathrm{y}(x^T x^i) + r)^d \tag{6}$$

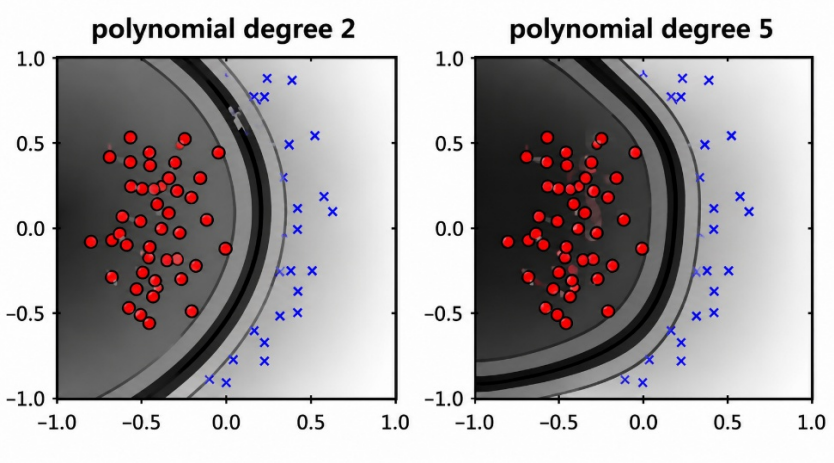

Fig. 4. Polynomial Kernel.

Fig. 4 shows that the degree of the polynomial kernel affects the flexibility of the decision boundary. A higher degree makes the model more flexible, but if the degree is too high, it can cause overfitting, where the model becomes overly tailored to the training data, leading to reduced accuracy on new, unseen data [39].

- RBF (Radial Basis Function) Kernel

  The RBF kernel is used to handle various types of data with efficient computation, resulting in accurate values. The RBF kernel is calculated using Equation 7.

$$K(x, x^{\mathrm{i}}) = \exp(-\mathrm{y}||x - x^i||^2) \tag{7}$$

As shown in Fig. 5, smaller gamma values (left panel) result in decision boundaries similar to linear SVMs. In contrast, larger gamma values (right panel) cause the decision boundary to be heavily influenced by the support vectors, potentially leading to overfitting.

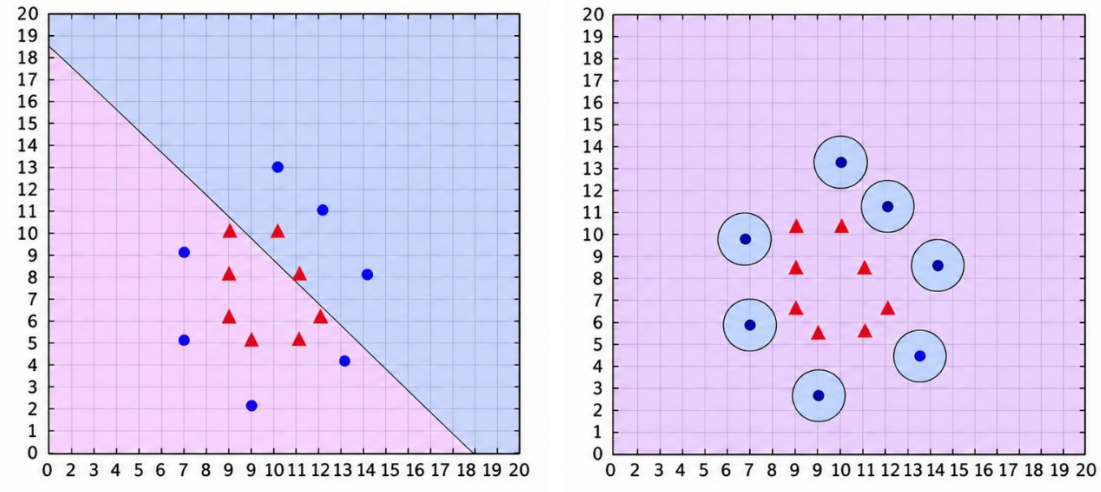

Fig. 5. RBF Kernel.

- Sigmoid Kernel

  The sigmoid kernel is a type of kernel that activates artificial neurons based on the derivative of a neural network [30]. The sigmoid kernel is calculated using Equation 8.

$$K(x, x^{\mathrm{i}}) = \tanh(\mathrm{y}(x^T x^i) + r) \tag{8}$$

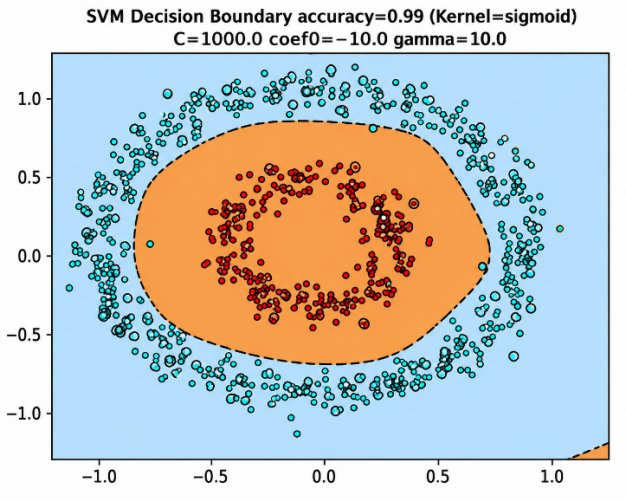

Fig. 6. Sigmoid Kernel.

Fig. 6 shows that too large a gamma value on the sigmoid kernel can lead to a decrease in classification accuracy, although this depends on the number of features used. In particular, a larger number of features tends to correspond to a smaller gamma value, and vice versa [39]. Each kernel is used to train a model, which is then tested on a testing dataset. The objective of training with various kernels is to identify the optimal SVM model for classifying brain tumor MRI images. After model training, these models are subsequently evaluated on a held-out test set using a confusion matrix.

Although deep learning approaches such as Convolutional Neural Networks (CNNs) have demonstrated strong performance in medical image analysis, this study intentionally focuses on GLCM-based feature extraction combined with SVM classification. The objective of this work is not to compete with deep learning models, but to establish a controlled and interpretable evaluation framework for classical kernel-based learning under identical experimental conditions.

The GLCM method produces a compact and structured feature vector, making it well-suited for SVM models, which perform effectively in moderate-dimensional spaces. Compared to CNN architectures, SVM requires significantly lower computational resources, offers faster training time, and provides clearer interpretability of decision boundaries. Moreover, in scenarios with limited dataset size and computational infrastructure, traditional machine learning approaches remain practical, stable, and reproducible alternatives. Therefore, this study focuses on systematically evaluating SVM kernel behavior within a controlled texture-feature setting, while deep learning-based comparisons may be explored in future research.

2.5. Model Evaluation

The model evaluation stage is the final stage of this research, where GLCM-SVM models that have been trained with linear, polynomial, RBF, and sigmoid kernels are compared to determine the most effective kernel and determine the best parameter combination for data classification. The evaluation is done using the main metric of the confusion matrix.

The confusion matrix is used to evaluate the performance of the prediction method by measuring the accuracy of the classification process. By comparing the model prediction with the actual value of the test data, the confusion matrix will show how the classification model performs. In the evaluation

stage, several experiments will be conducted involving the GLCM-SVM algorithm. This research will employ a confusion matrix to evaluate the accuracy, precision, recall, F1-score of various kernels [40], [41].

3. Results and Discussion

In this study, the test scenario involved splitting the dataset into two parts: training data and test data, with an 80:20 ratio. This resulted in 2240 images for training and 560 images for testing. This division aims to ensure that the model can effectively learn from the training and testing data, resulting in optimal results. The images are then pre-processed and subjected to GLCM feature extraction using a variety of angles to determine the angles that provide the highest accuracy. Four GLCM features, namely energy, contrast, correlation, and homogeneity, were used in this study. Each scenario was tested on a different SVM kernel to compare which kernel was optimal for the study.

3.1. GLCM Test Result

In this study, GLCM parameter evaluation consisted of two experiments: angular variation and distance variation. The angular experiment assessed different orientation parameters (θ) in the formation of the GLCM matrix to identify configurations that capture representative texture characteristics. Four orientations were tested: 0°, 45°, 90°, and 135°. Distance variation was also examined to analyze spatial relationships at different pixel separations (d = 1, 2, and 3). The results of these combinations are presented in Table 1.

Table 1 presents the "Average Score" obtained for each distance–angle combination. The "Average Score" represents the mean aggregated value of the four extracted GLCM features (energy, contrast, correlation, and homogeneity) computed across all training images. Prior to aggregation, feature values were kept in their computed scales, and for each MRI image, the four features were summed to obtain a combined texture magnitude indicator. These values were then averaged across the dataset to provide a comparative reference for each parameter configuration. It should be emphasized that this aggregated score does not directly represent classification performance. Instead, it serves as an exploratory indicator of overall texture intensity under different GLCM parameter settings. The final evaluation of model effectiveness was determined exclusively based on SVM classification results on the held-out test set.

Table 1. GLCM Combination Test Results.

Combination		Average Score
Distance	Angle	
1	0°	275.2774
1	45°	461.8387
1	90°	341.4619
1	135°	465.0850
2	0°	532.0614
2	45°	461.8387
2	90°	600.1222
2	135°	465.0850
3	0°	644.7587
3	45°	705.0052
3	90°	775.6530
3	135°	716.2338

As shown in Table 1, for distance = 1, the highest score was obtained at angle 135° (465.0850), while the lowest occurred at angle 0° (275.2774). For distance = 2, angle 90° produced the highest score (600.1222). For distance = 3, the combination of angle 90° yielded the highest overall score (775.6530), followed by angle 135° (716.2338). Based on this comparative analysis, the configuration of distance = 3 and angle = 90° was selected for the classification stage as it exhibited the most prominent aggregated texture response among the tested combinations. However, model performance validation relied solely on classification metrics rather than feature magnitude alone.

To further illustrate the statistical behavior of the selected configuration (distance = 3, angle = 90°), Fig. 7 presents the mean feature values for both tumor and non-tumor classes, along with their variability. The bar chart shows the distribution of the four GLCM features energy, contrast, homogeneity, and correlation computed under the selected parameter setting.

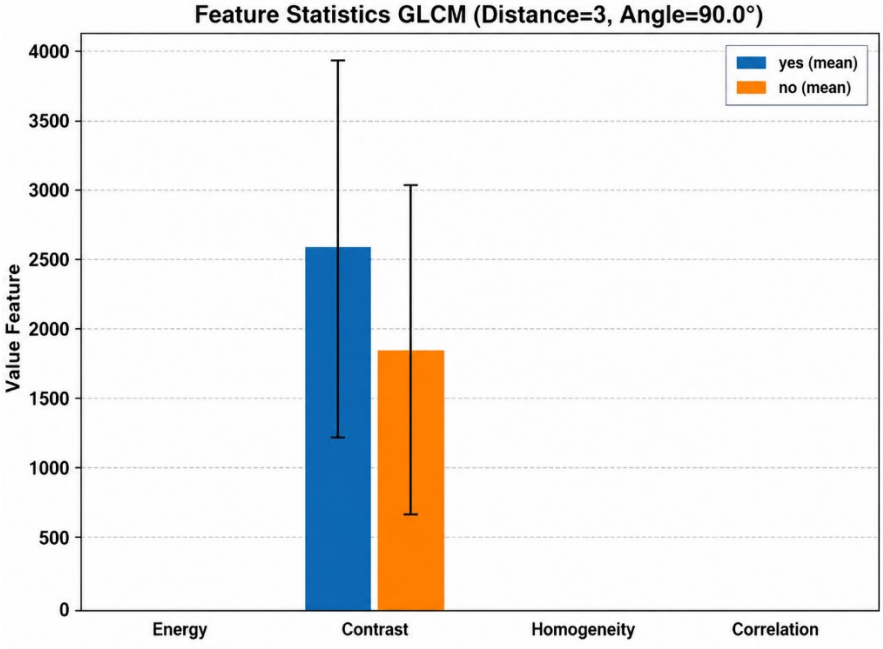

Fig. 7. Mean GLCM feature values (distance = 3, angle = 90°) for tumor and non-tumor classes. Error bars indicate standard deviation across images.

As shown in Fig. 7, the contrast feature exhibits the most pronounced difference between tumor and non-tumor classes, with higher mean values observed in tumor images. This suggests that tumor regions generate stronger intensity variations compared to normal brain tissue. In contrast, energy, homogeneity, and correlation display relatively smaller differences between classes, indicating that contrast plays a more dominant role in distinguishing texture irregularities in this configuration. The observed separation in feature statistics supports the suitability of the selected GLCM parameters prior to classification, although final performance evaluation was determined by SVM-based metrics.

3.2. SVM Test Result

After obtaining the GLCM distance and angle values, the next step is to evaluate the SVM model. This evaluation is done to assess the model's ability to classify brain tumor images. This test involves four SVM kernels: linear, polynomial, radial basis function (RBF), and sigmoid. Each kernel uses various parameters to determine the optimal parameter combination that produces the highest accuracy. For each kernel, several combinations of c, gamma, and degree parameters were tested to identify the optimal configuration that maximizes classification accuracy Table 2 presents the combinations of c, gamma, and degree parameters used in this study.

The C parameter balances margin width and training error, with smaller C favoring wider margins and larger C prioritizing correct classification. Gamma controls the impact of individual data points in non-linear kernels. A high gamma value results in a very tight decision boundary, which can lead to overfitting, whereas a low gamma produces a smoother and simpler boundary but may result in underfitting. The polynomial kernel's degree parameter determines the complexity of the decision boundary. A lower degree results in a simpler model, while a higher degree creates a more complex model, potentially leading to overfitting. Optimizing C, gamma, and degree is essential for achieving a balanced model that accurately captures patterns without compromising generalization.

Table 2. SVM Kernel Parameters.

Kernel	Parameters		
	C	*Gamma*	*Degree*
Linear	0.1, 1, 10, 100, 1000	-	-
Polynomial	0.1, 1, 10, 100	0.001, 0.01, 0.1, 1	2, 3, 4, 5
Radial Basis Function (RBF)	0.01, 0.1, 1, 10, 100	0.001, 0.01, 0.1, 1, 10	
Sigmoid	0.1, 1, 10, 100, 1000	0.001, 0.01, 0.1, 1, 10	

3.2.1. Linear Kernel Test Result

For the linear kernel, this experiment involves testing five different values of the C parameter: 0.1, 1, 10, 100, and 1000. These various C values were used to determine the optimal parameter that yielded the highest accuracy. The search for the optimal C parameter was conducted using the RandomizedSearch CV library. Randomized Search CV is a function that is useful for randomly searching for the best hyperparameters from a given set of parameters.

Fig. 8 shows the accuracy testing results of the linear kernel, indicating that increasing the value of parameter C initially improves accuracy, from around 69% at C = 0.1 to stabilizing at approximately 72% at C = 10 and beyond. The optimal value of C is C = 10, as further increases do not lead to significant changes in accuracy. This stability occurs because the linear kernel can only capture linear relationships between features, so increasing C does not enhance the model's flexibility. The resulting accuracy is largely limited by the linear patterns in the data and the quality of the features used.

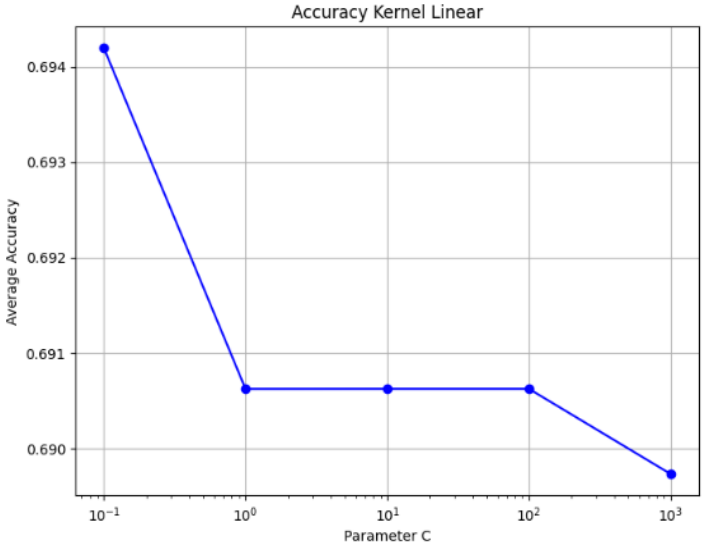

Fig. 8. Linear Kernel Accuracy Results.

3.2.2. Polynomial Kernel Test Result

The polynomial kernel was tested using various combinations of C, degree, and gamma parameters. The C parameter values used were (0.1, 1, 10, 100), the degree parameter values were (2, 3, 4), and the gamma parameter values were (0.001, 0.01, 0.1, 1). Using these combinations allowed for a broader exploration to find the optimal parameter configuration. The polynomial kernel parameter tuning was performed using GridSearchCV. GridSearchCV is a method for selecting the best combination of model and hyperparameters by exhaustively testing all possible combinations and validating each combination. The goal is to determine the combination that results in the best model performance for prediction.

Fig. 9 illustrates the accuracy of the polynomial kernel model based on combinations of the parameters C, degree, and gamma. In general, accuracy increases as the gamma value grows, with the best combination being C:10, degree:2, and gamma:1, yielding an accuracy of approximately 70%.

Conversely, a small gamma value (0.001) results in an accuracy of around 50%, indicating the model's failure to effectively learn patterns.

The increase in accuracy with higher gamma values occurs because gamma controls the model's sensitivity to the data. A small gamma value makes the model smoother, while a larger gamma allows the model to capture more detailed patterns. However, if gamma becomes too large, the risk of overfitting increases. A high C value and degree also need to be balanced to prevent the model from becoming overly complex.

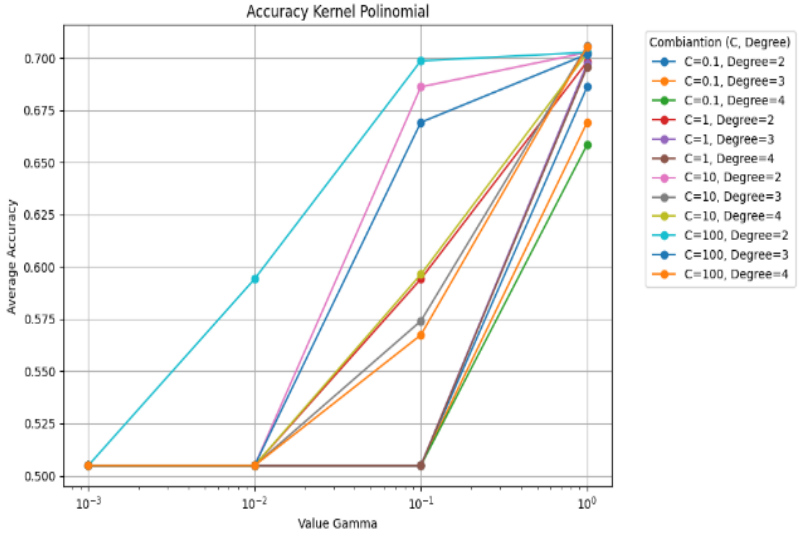

Fig. 9. Polynomial Kernel Accuracy Results.

3.2.3. RBF Kernel Test Result

In this research, the RBF kernel of the Support Vector Machine (SVM) was evaluated using various combinations of C and gamma parameters. The C parameter values were (0.01, 0.1, 1, 10, 100) and the gamma parameter values were (0.001, 0.01, 0.1, 1, 10). By varying these parameters, we can adjust how the model handles non-linear classification problems. The parameter tuning for the RBF kernel was performed using GridSearchCV. GridSearchCV is a method for selecting the best combination of model and hyperparameters by exhaustively testing all possible combinations and validating each combination. The goal is to determine the combination that results in the best model performance for prediction.

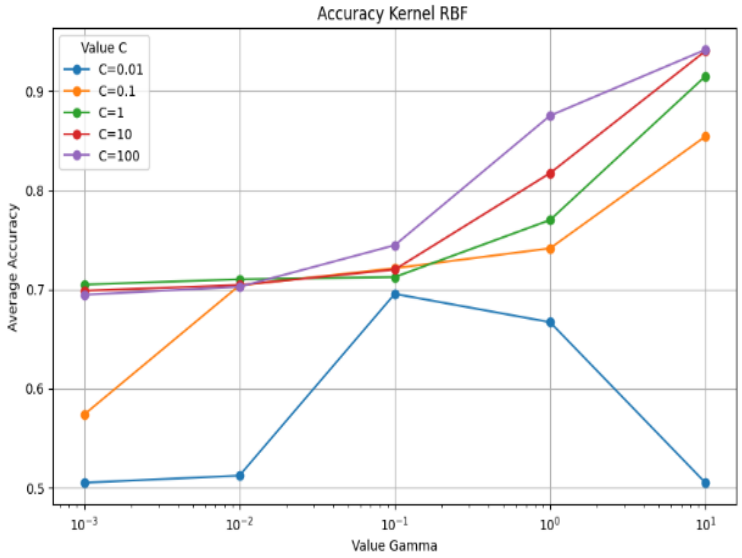

Fig. 10. RBF Kernel Accuracy Results.

Fig. 10 illustrates that the accuracy of the RBF kernel is affected by the combination of C and gamma values. In general, the results show that accuracy increases as both C and gamma grow larger. At lower C values (such as C = 0.1), the model produces moderate accuracy, particularly at small gamma values, because the decision boundary is still relatively simple. As C increases from 1 to 10, the accuracy improves significantly, especially at higher gamma values. This indicates that the model becomes more flexible in capturing complex data patterns while still maintaining generalization capability. The highest accuracy is achieved at C = 100 with large gamma, reaching approximately 95%. However, such high parameter values may increase the risk of overfitting because the model fits the training data very closely. Therefore, a more balanced and optimal combination is observed at C = 10 with large gamma (gamma=100), where the model achieves high accuracy while maintaining better generalization performance.

Small gamma values make the model too smooth, failing to capture complex patterns, while large gamma values help the model map the patterns well, although the risk of overfitting increases. A large C value narrows the decision margin, increasing the model's sensitivity to the data, while a small C value makes the model less sensitive to the details.

3.2.4. Sigmoid Kernel Test Result

The sigmoid kernel of the Support Vector Machine (SVM) was evaluated using various combinations of C and gamma parameters. The C parameter values were (0.1, 1, 10, 100) and the gamma parameter values were (0.001, 0.01, 0.1, 1, 10). By varying these parameters, we can adjust how the model handles non-linear classification problems. The parameter tuning for the sigmoid kernel was performed using GridSearchCV. GridSearchCV is a method for selecting the best combination of model and hyperparameters by exhaustively testing all possible combinations and validating each combination. The goal is to determine the combination that results in the best model performance for prediction.

Fig. 11 shows the accuracy of the sigmoid kernel based on the combination of parameters C and gamma. Overall, accuracy increases with smaller gamma values (gamma: 0.01 and gamma: 0.1), with a larger C value (C: 100) yielding the highest accuracy of around 71%. However, when gamma is too large (gamma: 1 and gamma: 10), accuracy drops significantly for all values of C.

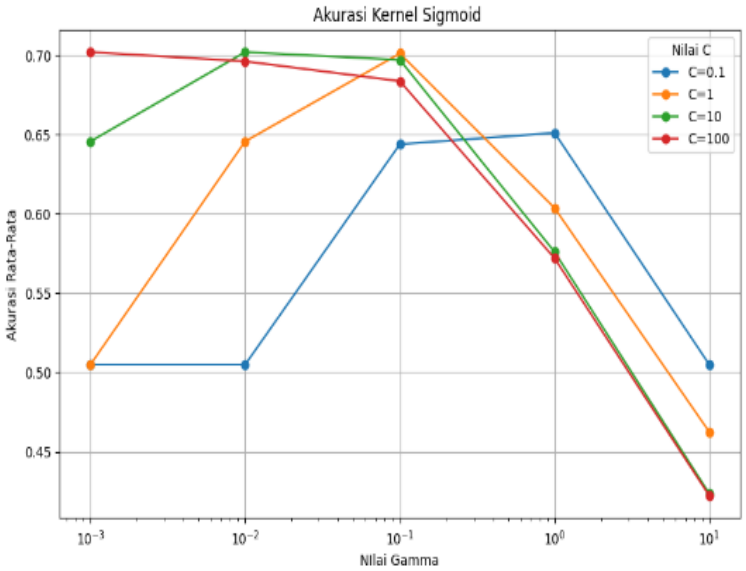

Fig. 11. Sigmoid Kernel Accuracy Results.

This occurs because smaller gamma values make the decision function smoother, allowing the model to capture patterns moderately. With a moderate gamma, the model can capture more complex patterns without being overly specific, resulting in optimal accuracy. In contrast, a larger gamma makes the decision function too sensitive to the data, leading to overfitting and reduced accuracy. A larger C value helps the model focus on the details of the patterns, but there is a risk of overfitting if the gamma is not appropriately set.

From Table 3, it can be observed that the RBF kernel achieves the highest accuracy of 96% with parameters C:100 and gamma:10. Meanwhile, the linear kernel achieves an accuracy of 72% with parameters C:0.1. This is because the linear kernel can only capture linear relationships between features, making it less flexible for recognizing non-linear patterns in brain tumor images.

The polynomial kernel achieves an accuracy of 74% with parameters C:100, gamma:1, and degree:3. While the polynomial kernel can capture non-linear patterns, its performance depends on the degree of the polynomial. A degree that is too high can lead to overfitting, whereas a low degree might lack the complexity needed to model patterns in the data.

Table 3. Test Result Kernel SVM.

Kernel	Best Parameter	Accuracy
Linear	C: 0.1	72%
Polynomial	C:100 Gamma: 1 Degree: 3	74%
RBF	C: 100 Gamma: 10	96%
Sigmoid	C: 10 Gamma: 0.01	71%

Lastly, the sigmoid kernel achieves an accuracy of 71% with parameters C:10 and gamma:0.01. The sigmoid kernel is often used as an activation function in neural networks but does not always perform optimally in SVM. It tends to be sensitive to the parameters C and gamma and is prone to underfitting, making it less effective in separating complex data patterns. Although the RBF kernel demonstrates the highest classification performance, this finding is consistent with theoretical expectations for non-linear texture classification problems. Therefore, the main contribution of this study is not merely identifying the best-performing kernel, but demonstrating that the observed performance differences remain stable under identical preprocessing pipelines, GLCM feature configurations, and hyperparameter search spaces. By ensuring methodological consistency across all experiments, this study provides a controlled and reproducible benchmarking framework for evaluating SVM kernels in brain tumor MRI classification. To further ensure robustness, hyperparameter tuning was performed using GridSearchCV, and model performance was evaluated exclusively on a held-out test set to prevent data leakage.

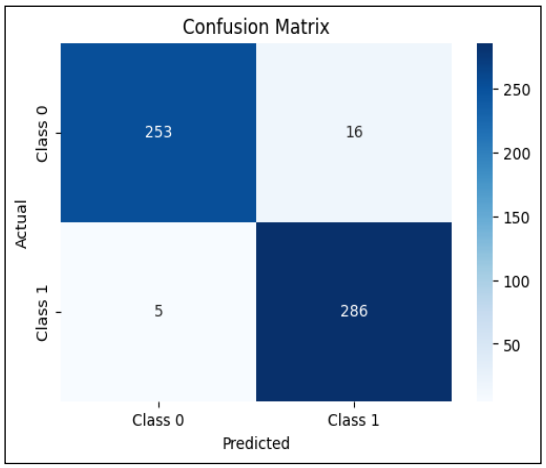

Fig. 12. Confusion Matrix RBF Kernel.

The confusion matrix above shows the evaluation results for the RBF kernel. This kernel is able to classify the data well. However, there are still some misclassifications, with 16 instances of class 0 (no tumor) wrongly identified as class 1 (tumor), and 5 instances of class 1 (tumor) incorrectly classified as class 0 (no tumor). These results indicate that the model's performance can still be improved.

The model's performance, evaluated using an RBF kernel to distinguish between Tumor and No-Tumor classes, is presented in Table 4. The model achieved an average accuracy, precision, recall, and F1-Score of 96% across both classes, demonstrating a reliable and balanced performance.

In addition to accuracy, precision, recall, and F1-score, the model performance can also be interpreted in terms of sensitivity and specificity derived from the confusion matrix. These metrics provide further insight into the trade-off between false positives and false negatives, which is particularly important in medical image classification. Although ROC-AUC was not explicitly computed in this study, the confusion matrix-derived metrics indicate strong discriminative capability of the RBF-based model in distinguishing tumor and non-tumor images.

Table 4. Confusion Matrix RBF Kernel.

Class	Accuracy	Precision	Recall	F1-Score
Tumor	0,96	0,95	0,98	0,96
No-Tumor	0,96	0,98	0,94	0,96
Average	0,96	0,96	0,96	0,96

Fig. 13 presents the ROC–AUC evaluation of the best-performing RBF model. The ROC curve illustrates the trade-off between the True Positive Rate (sensitivity) and False Positive Rate across different classification thresholds. The model achieved an AUC value of 0.962, indicating excellent discriminative capability in distinguishing between Tumor and No-Tumor classes. The curve's proximity to the top-left corner suggests that the classifier maintains high sensitivity while controlling the false positive rate. This result confirms that the RBF kernel demonstrates strong performance not only in threshold-based metrics such as accuracy and F1-score but also in threshold-independent evaluation. Furthermore, k-fold cross-validation results reinforce this finding, with a mean accuracy of 0.96, a standard deviation of 0.0063, and a 95% confidence interval ranging from 0.9512 to 0.9688. These results indicate consistent and stable model performance across different data partitions. Therefore, the ROC–AUC analysis, supported by cross-validation stability, strengthens the reliability of the RBF model as the most effective classifier in this study.

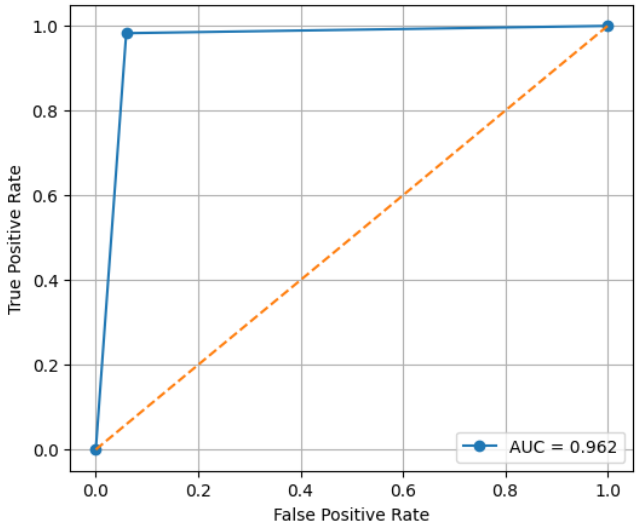

Fig. 13. Receiver Operating Characteristic (ROC) curve of the RBF-SVM classifier showing an AUC of 0.962 for binary brain tumor classification.

Overall, the evaluation results demonstrate that the RBF kernel consistently outperforms other SVM kernels across multiple performance metrics, including accuracy, F1-Score, ROC–AUC, and cross-validation stability. The combination of high discriminative ability and low performance variability indicates that the model generalizes well to unseen data. These findings confirm that the RBF kernel is the most suitable configuration for brain tumor MRI classification in this study and provides a reliable foundation for subsequent analysis and potential clinical decision-support applications.

3.2.5. Clinical Implication

From a clinical perspective, false negatives and false positives carry distinct and significant consequences. False negatives, in which tumor cases are misclassified as normal, may delay referral for further imaging, biopsy, or therapeutic intervention, allowing potential tumor progression and adversely affecting prognosis. In contrast, false positives may result in unnecessary follow-up MRI examinations, additional diagnostic procedures, increased healthcare expenditure, and heightened patient anxiety. Therefore, deployment of automated screening systems requires careful balance between sensitivity and specificity to mitigate these asymmetric clinical risks.

In practical clinical workflows, particularly in high-volume MRI screening environments, the proposed GLCM–SVM framework may serve as a preliminary triage mechanism. By automatically flagging images with tumor-like texture characteristics, the system can assist radiologists in prioritizing cases that require immediate attention, potentially reducing diagnostic delays.

Given its relatively low computational requirement and compact feature representation, this approach is especially relevant in healthcare settings with limited computational infrastructure or restricted access to advanced deep learning systems. Importantly, the system is not intended to replace radiologists but to function as a decision-support tool that complements expert judgment, supports borderline cases, and contributes to more efficient case management.

4. Conclusion

The study found that the GLCM–SVM combination yielded promising results, with varying accuracies across different kernels. The linear kernel achieved a peak accuracy of 72% with C = 0.1, the polynomial kernel reached 74% with C = 100, degree = 3, and gamma = 1, the RBF kernel attained the highest accuracy of 96% with C = 100 and gamma = 10, and the sigmoid kernel achieved 71% with C = 10 and gamma = 0.01. While the RBF kernel demonstrated the highest performance, the primary value of this study lies in the structured and controlled benchmarking framework that enables fair and transparent kernel comparison. The results confirm that under identical preprocessing, feature extraction, and hyperparameter tuning conditions, non-linear kernels are better suited for texture-based MRI tumor classification. The consistent performance patterns observed across experiments further reinforce the robustness and reproducibility of the proposed evaluation framework. Future research may extend this framework by incorporating multi-angle feature aggregation strategies, expanded validation schemes such as cross-validation, and comparative analysis with deep learning architectures to further assess generalizability and computational trade-offs.

Acknowledgment

The Research/Writing Team would like to express their gratitude to the Centre for Data Science and Sustainable Technologies, INTI International University, Negeri Sembilan, Malaysia, for the funding plan for the publication accepted in the targeted journal. The Research Team/Authors also extend their gratitude to the Research and Community Service Institute of UPN Veteran Jakarta and UPN Veteran East Java for the research facilities provided, as well as the Ministry of Higher Education, Science, and Technology of the Republic of Indonesia for its research grant.

Declarations

Author contribution. The following are the contributions of each author, including: Kraugusteeliana (Conceptualization, Methodology, Supervision, Writing - Original Draft), I Gede Susrama Mas Diyasa (Conceptualization, Methodology, Supervision, Validation, Writing - Review & Editing), Hanif Nur Fadlilah (Software, Validation, Formal analysis, Project administration), Yisti Vita Via (Conceptualization, Methodology, Supervision, Writing - Original Draft) , Anita Muliawati (Validation, Investigation, Data Curation), Allan Ruhui Fatmah Sari (Software, Validation, Formal analysis, Project administration), Erna Harfiani (Validation, Investigation, Data Curation), Ni Made Ika Marini

Mandenni (Conceptualization, Methodology, Supervision), Deshinta Arrova Dewi (Conceptualization, Methodology, Supervision, Funding acquisition)

Funding statement. Centre for Data Science and Sustainable Technologies, INTI International University, Negeri Sembilan, Malaysia.

Conflict of interest. All authors declare that they have no conflict of interest in submitting to this journal.

Additional information. No additional information is available for this paper.

References

[1] A. Ginorio, "Organization of Central Office.," *Am. Psychol.*, vol. 29, no. 11, pp. 849–849, Nov. 1974, doi: 10.1037/h0038188.

[2] M. Sammons, M. C. Popescu, J. Chi, S. D. Liberles, N. Gogolla, and A. Rolls, "Brain-body physiology: Local, reflex, and central communication," *Cell*, vol. 187, no. 21, pp. 5877–5890, Oct. 2024, doi: 10.1016/j.cell.2024.08.050.

[3] M. Weller *et al.*, "Glioma," *Nat. Rev. Dis. Prim.*, vol. 10, no. 1, p. 33, May 2024, doi: 10.1038/s41572-024-00516-y.

[4] R. Rahman *et al.*, "DNA damage response in brain tumors: A Society for Neuro-Oncology consensus review on mechanisms and translational efforts in neuro-oncology," *Neuro. Oncol.*, vol. 26, no. 8, pp. 1367–1387, Aug. 2024, doi: 10.1093/neuonc/noae072.

[5] A. Delaidelli and A. Moiraghi, "Recent Advances in the Diagnosis and Treatment of Brain Tumors," *Brain Sci.*, vol. 14, no. 3, p. 224, Feb. 2024, doi: 10.3390/brainsci14030224.

[6] T. T. T. Nguyen, L. A. Greene, H. Mnatsakanyan, and C. E. Badr, "Revolutionizing Brain Tumor Care: Emerging Technologies and Strategies," *Biomedicines*, vol. 12, no. 6, p. 1376, Jun. 2024, doi: 10.3390/biomedicines12061376.

[7] I. Ilic and M. Ilic, "International patterns and trends in the brain cancer incidence and mortality: An observational study based on the global burden of disease," *Heliyon*, vol. 9, no. 7, p. e18222, Jul. 2023, doi: 10.1016/j.heliyon.2023.e18222.

[8] G. S. M. Diyasa, A. Fauzi, M. Idhom, and A. Setiawan, "Multi-face Recognition for the Detection of Prisoners in Jail using a Modified Cascade Classifier and CNN," *J. Phys. Conf. Ser.*, vol. 1844, no. 1, p. 012005, Mar. 2021, doi: 10.1088/1742-6596/1844/1/012005.

[9] L. Szilágyi and L. Kovács, "Special Issue: Artificial Intelligence Technology in Medical Image Analysis," *Appl. Sci.*, vol. 14, no. 5, p. 2180, Mar. 2024, doi: 10.3390/app14052180.

[10] S. Kordnoori, M. Sabeti, H. Mostafaei, and S. Seyed Agha Banihashemi, "Advances in medical image analysis: A comprehensive survey of lung infection detection," *IET Image Process.*, vol. 18, no. 13, pp. 3750–3800, Nov. 2024, doi: 10.1049/ipr2.13246.

[11] D. S. Raikwar and D. F. R. Rao, "Diagnostic Accuracy of CT Scan Versus MRI in Detecting Brain Tumors," *Int. J. Med. Pharm. Res.*, vol. 5, no. 5, Oct. 2024, Accessed: Jun. 27, 2026. [Online]. Available: https://ijmpr.in/article/diagnostic-accuracy-of-ct-scan-versus-mri-in-detecting-brain-tumors-666/.

[12] Ali Sayedain Jaffar *et al.*, "Comparative Analysis of MRI and CT Scan for the Diagnosis of Brain Tumor, Considering MRI as Gold Standard," *J. Heal. Wellness Community Res.*, vol. 3, no. 3, p. e106, Apr. 2025, doi: 10.61919/a82eqd69.

[13] A. Campion and M. Iv, "Brain Tumor Imaging: Review of Conventional and Advanced Techniques," *Semin. Neurol.*, vol. 43, no. 06, pp. 867–888, Dec. 2023, doi: 10.1055/s-0043-1776765.

[14] Y. X. Nishanova, M. A. Q. Alisherova, A. S. Saloni, Sajid Maner Arshaan, X. O. Toyirov Abbos, and A. T. O. Bekmuradov, "Role of Magnetic Resonance Imaging (MRI) in Evaluation of Brain Tumors," *Am. J. Med. Med. Sci.*, vol. 15, no. 2, pp. 337–345, 2025, Accessed: Jun. 27, 2026. [Online]. Available: http://article.sapub.org/10.5923.j.ajmms.20251502.16.html

[15] N. Elazab, W. Gab Allah, and M. Elmogy, "Computer-aided diagnosis system for grading brain tumor using histopathology images based on color and texture features," *BMC Med. Imaging*, vol. 24, no. 1, p. 177, Jul. 2024, doi: 10.1186/s12880-024-01355-9.

[16] P. A. Riyantoko, Sugiarto, I. G. S. M. Diyasa, and Kraugusteeliana, "F.Q.A.M' Feyn-QLattice Automation Modelling: Python Module of Machine Learning for Data Classification in Water Potability," in *2021 International Conference on Informatics, Multimedia, Cyber and Information System (ICIMCIS*, IEEE, Oct. 2021, pp. 135–141. doi: 10.1109/ICIMCIS53775.2021.9699371.

[17] M. Mehdipor Ghazvini, V. Dehlaghi, A. Papi, and M. Siyah Mansoory, "Diagnosis and Classification of Brain Tumors from MRI Images Using the SVM Algorithm," *J. Clin. Res. Paramed. Sci.*, vol. 13, no. 1, p. e148703, Aug. 2024, doi: 10.5812/jcrps-148703.

[18] O. Farghaly and P. Deshpande, "Texture-Based Classification to Overcome Uncertainty between COVID-19 and Viral Pneumonia Using Machine Learning and Deep Learning Techniques," *Diagnostics*, vol. 14, no. 10, p. 1017, May 2024, doi: 10.3390/diagnostics14101017.

[19] Y. Li, Z. Zhou, Q. Feng, and H. Li, "Analysis and Comparison of Machine Learning-Based Facial Expression Recognition Algorithms," *Algorithms*, vol. 18, no. 12, p. 800, Dec. 2025, doi: 10.3390/a18120800.

[20] O. K. Xin, W. Wider, and L. K. Ling, "Human Resource Artificial Intelligence Implementation and Organizational Performance in Malaysia," *Asia-Pacific Soc. Sci. Rev.*, vol. 22, no. 3, p. 3, Sep. 2022, doi: 10.59588/2350-8329.1461.

[21] I. Malashin, V. Tynchenko, A. Gantimurov, V. Nelyub, and A. Borodulin, "Support Vector Machines in Polymer Science: A Review," *Polymers (Basel).*, vol. 17, no. 4, p. 491, Feb. 2025, doi: 10.3390/polym17040491.

[22] Y. Lu and C. Yang, "Influence of GLCM texture parameters on lithological mapping using Sentinel-1 imagery," *Geocarto Int.*, vol. 39, no. 1, Jan. 2024, doi: 10.1080/10106049.2024.2425183.

[23] R. Jalloul, H. K. Chethan, and R. Alkhatib, "A Review of Machine Learning Techniques for the Classification and Detection of Breast Cancer from Medical Images," *Diagnostics*, vol. 13, no. 14, p. 2460, Jul. 2023, doi: 10.3390/diagnostics13142460.

[24] S. Saifullah and R. Dreżewski, "Advanced Medical Image Segmentation Enhancement: A Particle-Swarm-Optimization-Based Histogram Equalization Approach," *Appl. Sci.*, vol. 14, no. 2, p. 923, Jan. 2024, doi: 10.3390/app14020923.

[25] "Optimization of Gray Level Co-occurrence Matrix (GLCM) Texture Feature Parameters in Determining Rice Seed Quality," *Politek. Elektron. Negeri Surabaya*, vol. 13, no. 1, 2025, [Online]. Available: https://garuda.kemdiktisaintek.go.id/documents/detail/5299677.

[26] I. G. S. Masdiyasa, I. K. E. Purnama, and M. H. Purnomo, "A New Method To Improve Movement Tracking Of Human Sperms," *IAENG Int. J. Comput. Sci.*, vol. 45, no. 4, pp. 531–539, 2018, [Online]. Available: https://www.iaeng.org/IJCS/issues_v45/issue_4/IJCS_45_4_05.

[27] R. Parameswaran, V. P. G. Sivabalan, S. Rajendran, and T. S. Jayaraman, "Performance Analysis of RIS Assisted Power Domain NOMA System with Discrete Phase Shifter," in *2023 International Conference on Signal Processing, Computation, Electronics, Power and Telecommunication (IConSCEPT)*, IEEE, May 2023, pp. 1–5. doi: 10.1109/IConSCEPT57958.2023.10170235.

[28] C. Nyasulu *et al.*, "A comparative study of Machine Learning-based classification of Tomato fungal diseases: Application of GLCM texture features," *Heliyon*, vol. 9, no. 11, p. e21697, Nov. 2023, doi: 10.1016/j.heliyon.2023.e21697.

[29] D. Indra, H. M. Fadlillah, Kasman, and L. B. Ilmawan, "Rice Texture Analysis Using GLCM Features," in *2021 International Conference on Electrical, Computer and Energy Technologies (ICECET)*, IEEE, Dec. 2021, pp. 1–5. doi: 10.1109/ICECET52533.2021.9698594.

[30] P. Purnawansyah *et al.*, "Comparative Study of Herbal Leaves Classification using Hybrid of GLCM-SVM and GLCM-CNN," *Ilk. J. Ilm.*, vol. 15, no. 2, pp. 382–389, Aug. 2023, doi: 10.33096/ilkom.v15i2.1759.382-389.

[31] R. Guido, S. Ferrisi, D. Lofaro, and D. Conforti, "An Overview on the Advancements of Support Vector Machine Models in Healthcare Applications: A Review," *Information*, vol. 15, no. 4, p. 235, Apr. 2024, doi: 10.3390/info15040235.

[32] M. Jabardi, "Support Vector Machines: Theory, Algorithms, and Applications," *Infocommunications J.*, vol. 17, no. 1, pp. 66–75, 2025, doi: 10.36244/ICJ.2025.1.8.

[33] W. Sholihah, A. S. Handayani, and Sarjana, "Revolutionizing Healthcare: Comprehensive Evaluation and Optimization of SVM Kernels for Precise General Health Diagnosis," *Sci. J. Informatics*, vol. 10,4, pp. 577–589, Nov. 2023, [Online]. Available: https://journal.unnes.ac.id/nju/sji/article/view/46430.

[34] A. Jalili, Z. Saleki, Y. A. Luo, F. Pan, A. X. Chen, and J. P. Draayer, "Performance of various kernel functions for mass prediction with support vector machine," *Eur. Phys. J. A*, vol. 61, no. 6, p. 143, Jun. 2025, doi: 10.1140/epja/s10050-025-01610-9.

[35] W. Y. Wong, T. Hai Sam, C. W. Too, and W. Fong Pok, "Software Quality Assurance Plan: Setting Quality Assurance Checkpoints within the Project Life Cycle and System Development Life Cycle," in *2022 IEEE 18th International Colloquium on Signal Processing & Applications (CSPA)*, IEEE, May 2022, pp. 214–219. doi: 10.1109/CSPA55076.2022.9782044.

[36] A. Kar, N. Nath, U. Kemprai, and Aman, "Performance Analysis of Support Vector Machine (SVM) on Challenging Datasets for Forest Fire Detection," *Int. J. Commun. Netw. Syst. Sci.*, vol. 17, no. 02, pp. 11–29, Feb. 2024, doi: 10.4236/ijcns.2024.172002.

[37] S. S. Prasetiyowati, S. Harini, J. Nur Fadila, and H. Fahlena, "Revealing the Impact of the Combination of Parameters on SVM Performance in COVID-19 Classification," *Int. J. Inf. Commun. Technol.*, vol. 10, no. 1, pp. 127–140, Jul. 2024, doi: 10.21108/ijoict.v10i1.965.

[38] Q. A. Hidayaturrohman and E. Hanada, "A Comparative Analysis of Hyper-Parameter Optimization Methods for Predicting Heart Failure Outcomes," *Appl. Sci.*, vol. 15, no. 6, p. 3393, Mar. 2025, doi: 10.3390/app15063393.

[39] A. Kurniasih and C. N. Previana, "Implementation of GridSearchCV to Find the Best Hyperparameter Combination for Classification Model Algorithm in Predicting Water Potability," *J. Artif. Intell. Eng. Appl.*, vol. 4, no. 2, pp. 1174–1182, Feb. 2025, doi: 10.59934/jaiea.v4i2.844.

[40] M. Agarwal, G. Rani, A. Kumar, P. K. K, R. Manikandan, and A. H. Gandomi, "Deep learning for enhanced brain Tumor Detection and classification," *Results Eng.*, vol. 22, no. June, p. 102117, Jun. 2024, doi: 10.1016/j.rineng.2024.102117.

[41] M. Aamir, Z. Rahman, U. A. Bhatti, W. A. Abro, J. A. Bhutto, and Z. He, "An automated deep learning framework for brain tumor classification using MRI imagery," *Sci. Rep.*, vol. 15, no. 1, p. 17593, May 2025, doi: 10.1038/s41598-025-02209-2.